



Research on the Propulsion Performance of Screw Propeller for Kelp Harvesting Vessel

Shiji Zheng¹, Yu'e Yang^{1,a*}, Zhenhua Wang^{2,b*}, Guanghui Liu¹, Jiaqi Han¹

¹College of Mechanical Engineering, University of Jinan, Jinan 250022, China

²Weihai Changqing Ocean Science & Technology Co., Ltd, Rongcheng 264399, China

^{a*}Corresponding author's e-mail: 18764727527@163.com

^{a*} Corresponding author's e-mail: 1261843387@qq.com

Abstract. In response to the high maneuverability demands of kelp harvesting vessels during row-changing operations, this study employs a screw propeller instead of traditional propellers as the propulsion device. To ensure that the screw propeller meets the requirements for kelp harvesting vessels, the study investigates the influence of structural parameters of the screw propeller on its propulsion performance. Using computational fluid dynamics (CFD) in combination with orthogonal experimental design, this study systematically investigates the effects of structural parameters on the hydrodynamic performance of the marine screw propeller. By analyzing the impact mechanisms of four factors—blade height (175-250 mm), lead (430-580 mm), number of helices (1-3), and number of turns (1-4)—on propulsion efficiency, the significance of each parameter is ranked as follows: number of helices > blade height > lead > number of turns. The optimal parameter combination is found to be a blade height of 450 mm, a lead of 430 mm, and a single-turn, single-helix structure, resulting in a propulsion efficiency of 27.26%. The findings provide a theoretical basis for the engineering optimization of marine screw propellers.

Keywords: Screw propeller; ANSYS simulation; Orthogonal tests; Propulsive efficiency

1 Introduction

Kelp farming is a vital pillar of China's marine economy [1]. With the expansion of farming scales, traditional manual harvesting methods can no longer meet the demands. Consequently, kelp harvesting vessels have become essential equipment [2]. Conventional ship propulsion systems, such as propellers and paddle wheels, offer relatively high propulsive efficiency. However, in the context of kelp farming, their large turning radii limit the maneuverability of harvesting vessels. In contrast, the screw propeller, with its parallel arrangement of two counter-rotating helices, can achieve zero-radius turns and omnidirectional movement, significantly enhancing maneuverability and steering responsiveness. It thus represents an ideal choice for kelp harvesting vessels.

At present, domestic and foreign scholars have conducted many studies on screw propellers. For example, Seo [3] found through orthogonal experiments that the propulsive performance is optimal when the inclination angle is 35 degrees and the blade height is 14 mm. Li [4] pointed out that the best traveling performance of the propulsion vehicle is achieved when the helix angle is 30° and the number of helices is 2. Xu [5] discovered through experiments that the thrust is maximized when the submersion depth of the screw cylinder is 0.9 times its diameter, and by optimizing the blade height and pitch, the propulsive efficiency can be increased to 34.09%.

Existing research has indicated that the structural parameters of a screw propeller, such as blade height, pitch, number of helical lines, and number of turns, have a significant impact on propulsion efficiency [6]. However, these studies have primarily focused on feeders and amphibious vehicles, with relatively little research on marine propellers. This research gap means that when designing the parameters of marine screw propellers, there is a lack of a systematic theoretical basis, and design often relies on experience. This experience-driven design approach not only consumes a significant amount of time and material resources but also tends to result in propellers with low efficiency that fail to meet practical requirements. This, in turn, restricts the technological advancement of kelp harvesting vessels.

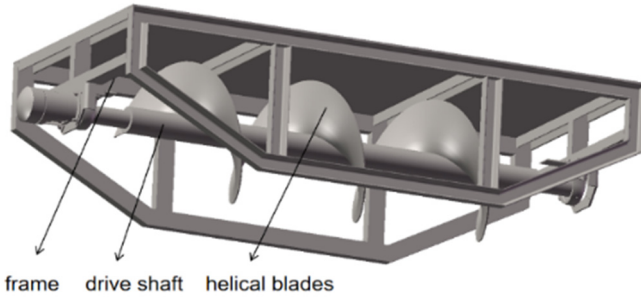
Therefore, this paper employs the Computational Fluid Dynamics (CFD) method and designs orthogonal experiments to systematically investigate the effects of blade height, number of helical lines, pitch, number of turns, and rotational speed of the screw propeller on thrust, torque, and propulsion efficiency of kelp harvesting vessels traveling at a speed of 0.5 m/s [7]. The aim is to provide a scientific basis for the design of helical propellers, optimize the parameter combinations to enhance propulsion efficiency, reduce operational costs, and thereby improve the economic benefits of the kelp farming industry.

2 Establishment of the Numerical Model for the Screw Propeller

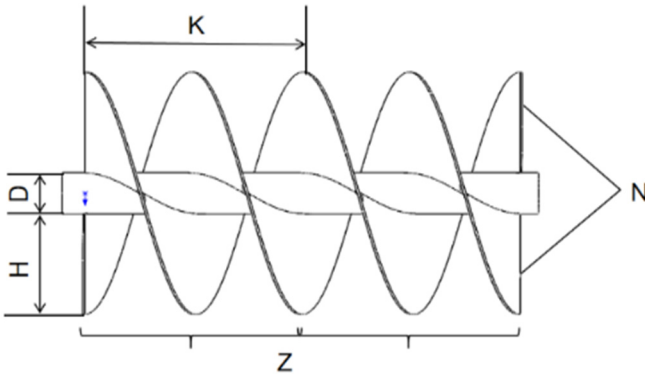
The screw propeller mainly consists of a frame, a drive shaft, and helical blades, as shown in Figure 1(a). Among these components, the helical blades, which serve as the primary thrust-generating elements of the propeller, have a decisive impact on the propulsion performance. This paper analyzes the structural parameters of the helical blades, mainly including blade height (H), lead (K), number of helices (N), and number of turns (Z), while keeping the diameter of the drive shaft (D) constant. Figure 1(b) shows a simplified structural diagram of the screw propeller with these parameters.

The screw propeller is to be applied to a kelp harvesting catamaran, with its size and thrust required to meet the operational needs of the harvesting vessel. The vessel is known to have a length of 12 meters, a width of 11 meters, a draft depth of 0.5 meters, an operating speed of 0.5 meters per second, and a travel resistance of 164.3 Newtons [8]. Based on the hull dimensions and power requirements, a prototype of the screw propeller has been preliminarily designed with the following structural parameters: blade height of 200 millimeters, helix number of 1, lead of 500 millimeters, and number

of turns of 1. At a rotational speed of 26 radians per second, it meets the travel requirements. To systematically investigate the influence of various factors on the propulsion performance of the spiral propeller while reducing the number of experiments, an orthogonal experimental design is employed. The experimental factors include blade height, helix number, lead, number of turns, and rotational speed, with the levels of each factor selected around the prototype parameters. The specific values are shown in Table 1:



(a)



(b)

Fig. 1. Model of a screw propeller and schematic diagram of its structure.

Table 1. A table of orthogonal test parameters.

	Blade height. A/mm	Lead B/mm	Helices C	Turns D	Rotational speed E/rad/s
1	200	480	3	1	21
2	175	530	1	1	26
3	250	430	2	3	36
4	225	580	4	2	31

Based on the orthogonal test table, SolidWorks software was used to establish 16 models of the screw propeller. The diameter D of the drive shaft was uniformly set to 100 mm. The blades were constructed by lofting two helical 3D sketches, ensuring that there were no gaps between the blades and the drive shaft. The 16 models are shown in Figure 2.

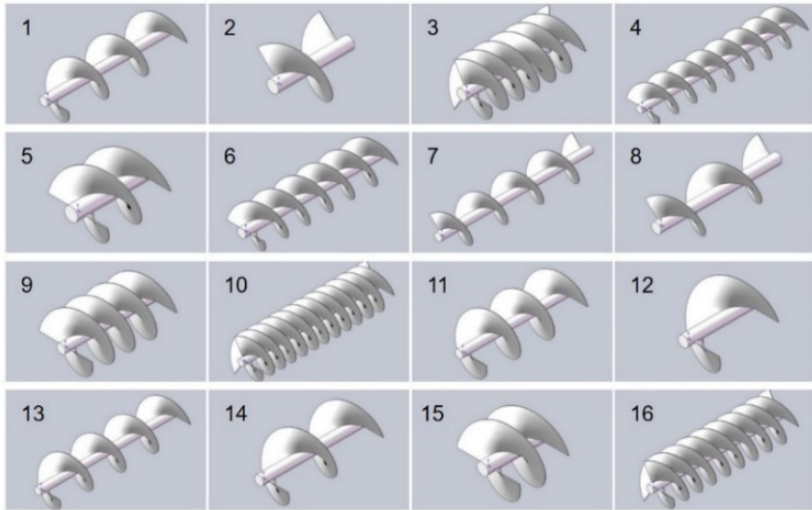


Fig. 2. Screw propeller simulation model.

3 Numerical Simulation Test

3.1 Computational Domain and Meshing

Based on the geometric shape of the screw propeller, the computational domain is designed as a cylinder to ensure simulation accuracy and computational efficiency. To avoid interference from the computational domain boundaries on the simulation results while reasonably conserving computational resources, the diameter of the computational domain is set to six times the diameter of the screw propeller ($6D$). The inlet boundary is positioned $4D$ from the leading edge of the screw propeller, and the outlet boundary is positioned $6D$ from the trailing edge, ensuring fully developed flow and minimizing boundary effects on the results. To simplify the computational model and improve efficiency, a physics-based suppression method is employed to ignore the solid part of the spiral propeller, retaining only its wall surfaces as computational boundaries. The specific layout of the computational domain is illustrated in Figure 3(a).

The mesh is automatically generated through Workbench. To avoid errors during the moving mesh solution process, the mesh orthogonality quality should be greater than 0.2. The global mesh size is set to 350 mm, and local mesh refinement is applied to the blade and its edge regions, as shown in Figure 3(b).

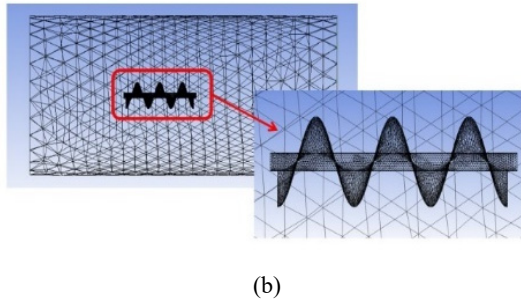
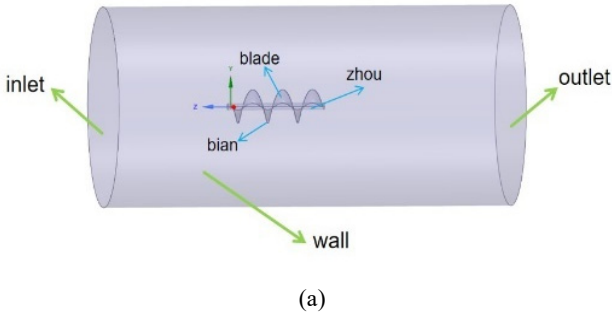


Fig. 3. Computational domain and meshing.

To investigate whether the number of mesh affects the simulation results, a mesh independence verification is required. The number of mesh directly impacts the accuracy of numerical simulations: too few mesh can lead to inaccurate results, while too many increase computational costs. For RANS (Reynolds-Averaged Navier-Stokes) simulations, the presence of turbulence models means that once the mesh density reaches a certain level, the results tend to stabilize, and further refinement does not significantly enhance accuracy[9]

Therefore, it is necessary to choose an appropriate number of mesh for calculations. Based on different meshing schemes, four models with varying numbers of mesh were generated and simulated. The converged thrust and torque results, along with their respective meshing schemes, are listed in Table 2. It can be seen from the table that there are no significant differences in the results among the four meshing schemes. To ensure computational accuracy while saving computational resources, the second meshing scheme was adopted for all simulations in this study.

Table 2. A table of mesh refinement scheme and results.

	Size Adjustment (bian/mm)	Size Adjustment (blade/mm)	Number of mesh.	Thrust (N)	Torque (Nm)
1	27	32	200,000	438.86	42.31
2	25	15	300,000	433.76	41.92
3	14	14	400,000	429.38	41.66
4	13	10	500,000	436.67	42.24

3.2 Controlling Equations and Turbulence Model

In order to reduce the complexity while ensuring the computational accuracy, the Reynolds Averaging Method (RANS) is used to describe the fluid motion. The RANS method is widely used in engineering to efficiently simulate the working process of a screw thruster by decomposing the flow into averaged and pulsating quantities.

To close the RANS equations, a turbulence model is introduced to calculate the Reynolds stresses. In this study, the SST $k-\omega$ turbulence model is used, which combines the advantages of the $k-\omega$ and $k-\varepsilon$ models, using the $k-\omega$ model for the near wall and the $k-\varepsilon$ model for the far wall, combining both high accuracy and wide applicability.

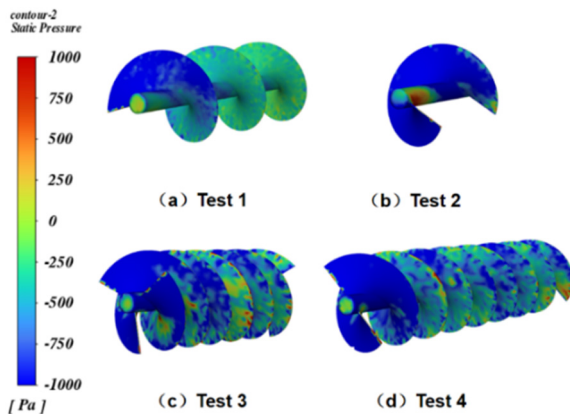
3.3 Boundary Conditions and Moving Mesh Settings

The fluid in the flow field is set as water, with velocity inlet and pressure outlet boundary conditions applied. The moving mesh is activated, with smoothing and remeshing options selected. A UDF is used to control the rotation of the screw propeller around the Z-axis. The center of gravity is positioned according to the model dimensions, and the cell height in the adjacent region is set to 350 mm. The PISO method is chosen for pressure-velocity coupling, and the spatial discretization of pressure is set to PRESTO.

4 Test Results and Analysis

4.1 Screw Propeller Blade Pressure Analysis

Taking the 1st, 2nd, 3rd, and 4th groups of tests as examples, the pressure on the blades of the screw propeller is analyzed. Figure 4(a) shows the pressure contour of the suction side of the screw propeller, while Figure 4(b) shows the pressure contour of the pressure side. The suction side refers to the blade surface facing the direction of motion, while the pressure side is the opposite side of the blade.



(a)

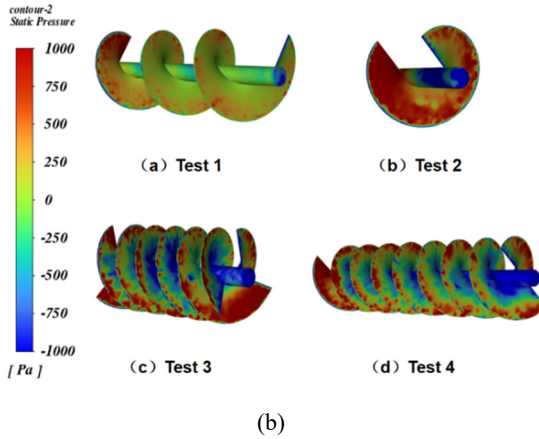


Fig. 4. Pressure distribution contours of the suction and pressure surfaces of a screw propeller.

As can be seen from Figure 4, the suction side of the screw propeller experiences negative pressure, while the pressure side experiences positive pressure. The pressure difference between these two sides is the source of the thrust generated by the screw propeller. As the rotational speed of the screw propeller increases, the pressure difference between the suction side and the pressure side also increases, thereby generating greater thrust.

For screw propellers with multiple helical turns, the first turn of blades facing the direction of motion experiences a higher-pressure load, meaning that the thrust is primarily generated by this first turn. Increasing the number of helical turns does not significantly enhance the thrust of the screw propeller.

For a single turn of the screw propeller blades, the outer part of the blades experiences a higher-pressure load. If the blade height is increased, the area at the blade edge will be enlarged, ultimately leading to an increase in thrust. Increasing the number of helices means that the pressure is generated collectively by all the blades. However, there is some interference between the blades, which results in a reduction in overall thrust. Additionally, an increase in the number of blades will lead to an increase in torque, which will ultimately reduce efficiency.

4.2 Orthogonal Test Analysis

The numerical simulation was conducted on the 16 models of the screw propeller, monitoring the thrust T and torque Q generated on the blades of the screw propeller. The propulsive efficiency η under each parameter combination was calculated using Equation (1), and the results are presented in Table 3.

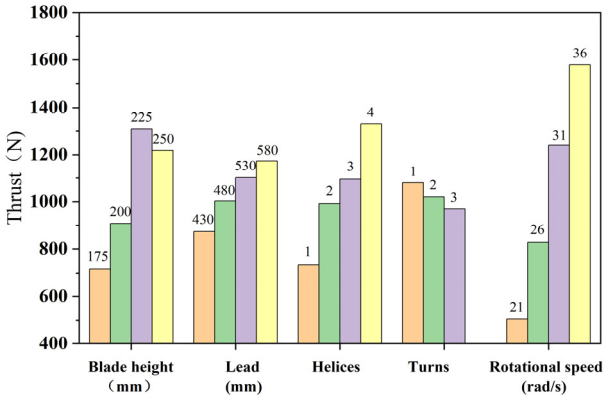
$$\eta = \frac{TV_A}{Qn} \times 100\% \quad (1)$$

In the formula: T- Thrust, N; Q- Torque, Nm; V_A -Speed, m/s; n- Rotational speed, rad/s

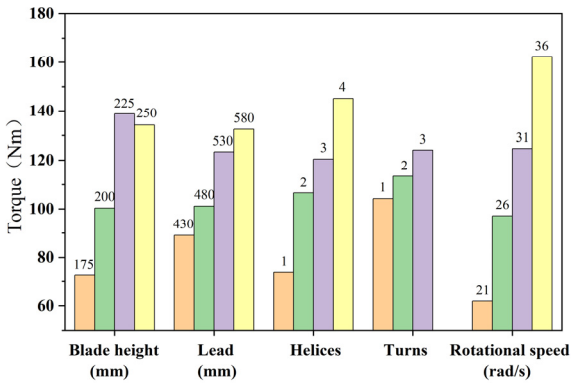
Table 3. A table of orthogonal test parameters.

Test	Blade height	Lead	Helices	Turns	Rotational	Thrust	Torque	Efficiency
	A/mm	B/mm	C	D	speed E/rad/s	T	Q	η
1	200	480	3	1	21	435.69	41.92	24.75%
2	200	530	1	1	26	505.02	53.13	18.28%
3	200	430	2	3	36	1167.85	136.37	11.89%
4	200	580	4	2	31	1521.73	170.08	14.43%
5	175	480	1	2	31	514.07	50.79	16.32%
6	175	530	3	2	36	1361.47	146.35	12.92%
7	175	430	4	1	26	671.14	62.16	20.76%
8	175	580	2	1	21	321.77	31.98	23.96%
9	250	480	2	2	26	910.22	106.27	16.47%
10	250	530	4	3	21	975.1	142.58	16.28%
11	250	430	3	1	31	1360.94	126.66	17.33%
12	250	580	1	1	36	1629.18	161.13	14.04%
13	225	480	4	1	36	2154.18	205.73	14.54%
14	225	530	2	1	31	1567.34	151.42	16.70%
15	225	430	1	2	21	290.01	31.06	22.23%
16	225	580	3	3	26	1224.08	166.88	14.11%

Conduct an extreme difference analysis on the thrust and torque of the propeller, and present the results in Figure 5. The numbers above each bar in the figure represent the level values of each factor, while the height differences between the bars reflect the degree of influence of each factor on thrust or torque. The greater the height difference, the more significant the influence. From the chart, it can be observed that the thrust and torque of the propeller increase with the increase in pitch, number of helical turns, and rotational speed, and they first increase and then decrease with the increase in blade height, with a peak existing between 200 mm and 250 mm. However, an increase in the number of helices will lead to a decrease in thrust but an increase in torque. The order of influence of each factor on thrust and torque is as follows: rotational speed > number of helical turns > blade height > pitch > number of helices.



(a)



(b)

Fig. 5. Histogram plot of the effect of each factor on thrust and torque.

Figure 6 presents the range analysis of the efficiency of the screw propeller. When efficiency is used as the indicator, a higher value indicates better propulsive performance of the screw propeller. It can be seen from the figure that the efficiency of the screw propeller decreases with the increase of blade height, lead, number of helices, and rotational speed, while the number of helical turns has no linear impact on it. The order of influence of each factor on the propulsive efficiency is: rotational speed > number of helices > blade height > lead > number of helical turns. The overall propulsive efficiency is highest when all factors are at their lowest levels, that is, when the blade height is 175 mm, the lead is 430 mm, the number of helical turns and the number of helices are both 1, and the rotational speed is 21 rad/s.

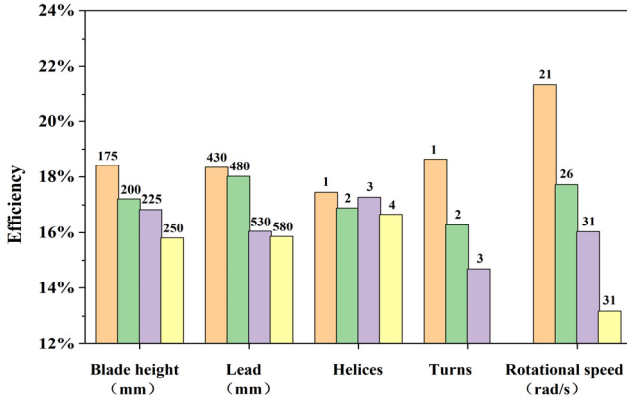


Fig. 6. Pressure distribution contours of the suction and pressure surfaces of a screw propeller.

Based on the parameter combination of the optimal efficiency solution, a screw propeller model was established, as shown in Figure 7(a). The same numerical simulation was performed, and the changes in thrust and torque were recorded, as shown in Figure 7(b). The data from 9 to 10 seconds were taken as the effective values. Under this parameter setting, the thrust of the screw propeller was calculated to be 168.4 N, and the torque was 14.7 Nm, which meets the requirements for the ship's propulsion. At this time, the propulsive efficiency was 27.27%.

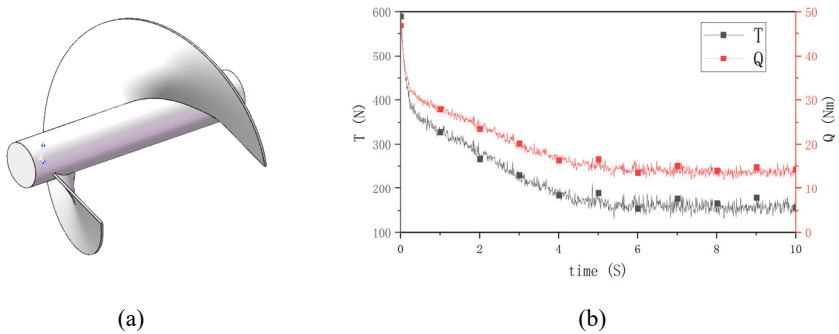


Fig. 7. Optimally structured screw propeller and its simulation results.

5 Conclusion

This paper investigates the propulsive performance of the screw propeller by varying five parameters—blade height, lead, number of helical turns, number of helices, and rotational speed—using orthogonal test design under given operating conditions. The propulsive efficiency is used as the criterion to select the optimal parameter combination, leading to the following conclusions:

(1) The influence of each parameter on the propulsive efficiency of the screw propeller, in descending order of significance, is as follows: rotational speed > number of helices > blade height > lead > number of helical turns. The optimal combination is: blade height of 175 mm, lead of 480 mm, one helical turn, one helix, and rotational speed of 21 rad/s. Under this combination, the highest efficiency is achieved at 27.26%. This finding provides a clear optimization direction for the design of screw propellers, especially in application scenarios that require efficient propulsion, such as underwater robots and ship propulsion systems.

(2) The propulsive efficiency of the screw propeller decreases with higher blade height, lead, number of helices, and rotational speed, while the number of helical turns has no linear effect. Increasing lead, helical turns, and rotational speed, however, boosts thrust and torque. This allows designers to balance efficiency and thrust based on needs. For high-thrust applications like heavy transport or emergency rescue, sacrificing some efficiency for greater thrust holds significant practical value.

(3) The results of this study not only provide a theoretical basis for the optimal design of spiral propellers, but also provide new ideas for further exploration of parameter optimization under different operating conditions in the future, in addition, these findings can be applied to other propulsion systems such as air propellers and wind turbines, which have a wide range of engineering applications.

Acknowledgments

This work was financially supported by the key research and development project in Shandong Province (2022CXGC020410).

References

1. Wang Bin (2024). Innovation and Integration: The Establishment of China's Seaweed Farming Technology System in the 1950s Ancient and Modern Agriculture (02), 1-16
2. Wang Jiayi (2024-01-09). The kelp industry links the ecological chain and wealth chain China Food News, 006. doi: 10.28137/n.cnki.ncspb.2024.000051.
3. Seo, C., Lee, K., Son, D., & Seo, T. (2021). Robust design of a screw-based crawling robot on a granular surface. *IEEE Access*, 9, 103988-103995.
4. Li Lutian, Xu Lei, Li Jun, Luo Peng&Chen Liubo (2024). The influence of spiral structure parameters on the driving performance of spiral propulsion vehicles *Agricultural Equipment and Vehicle Engineering* (07), 56-61
5. Xu Pengfei, Wang Zipeng, Lin Hailong, Kai Yan, Hu Qiao&Su Jianye (2024). Research on the Spiral Propulsion Performance of Amphibious Robots *Journal of Underwater Unmanned Systems* (06), 1063-1071
6. Miao, J., Li, X., Liang, B., Wang, J., & Xu, X. (2021). Enhancing swimming performance by optimizing structure of helical swimmers. *Sensors*, 21(2), 494.
7. Arina, I. M., Iswantoro, A., & Fitri, S. A. (2023). Combining Optimum Propeller Design on Roro Ship Re-engine. *Kapal: Jurnal Ilmu Pengetahuan dan Teknologi Kelautan*, 20(2), 201-2013.

8. Menter, F. R. (1994). Two-equation eddy-viscosity turbulence models for engineering applications. *AIAA Journal*, 32(8), 1598–1605.
9. Feng Jing'an, Tang Xiaoqi, Wang Weibing, Ying Rui&Zhang Ting (2017). Verification method for numerical simulation reliability based on grid independence and time independence *Journal of Shihezi University (Natural Science Edition)* (01), 52-56. doi: 10.13880/j.cnki.65-1174/n.2017.01.009.
10. Wang Tongshan (2023). Overall Design and Propulsion Performance Research of Kelp Harvesting Platform (Master's Thesis, Shandong Jiaotong University) Master <https://link.cnki.net/doi/10.27864/d.cnki.gsjtd.2023.000127>doi:10.27864/d.cnki.gsjtd.2023.000127.

Open Access This chapter is licensed under the terms of the Creative Commons Attribution-NonCommercial 4.0 International License (<http://creativecommons.org/licenses/by-nc/4.0/>), which permits any noncommercial use, sharing, adaptation, distribution and reproduction in any medium or format, as long as you give appropriate credit to the original author(s) and the source, provide a link to the Creative Commons license and indicate if changes were made.

The images or other third party material in this chapter are included in the chapter's Creative Commons license, unless indicated otherwise in a credit line to the material. If material is not included in the chapter's Creative Commons license and your intended use is not permitted by statutory regulation or exceeds the permitted use, you will need to obtain permission directly from the copyright holder.

